Two-dimensional dielectrophoretic particle trapping in a hybrid crystal/PDMS-system

Michael Esseling, Frank Holtmann, Mike Woerdemann, and Cornelia Denz

Institute for Applied Physics, Westfälische Wilhelms-Universität, Corrensstraße 2/4, 48149 Münster, Germany

michael.esseling@uni-muenster.de

Abstract: Dielectrophoretic forces originating from highly modulated electric fields can be used to trap particles on surfaces. An all-optical way to induce such fields is the use of a photorefractive material, where the fields that modulate the refractive index are present at the surface. We present a method for two-dimensional particle alignment on an optically structured photorefractive lithium niobate crystal. The structuring is done using an amplitude-modulating spatial light modulator and laser illumination. We demonstrate trapping of uncharged graphite particles in periodic and arbitrary patterns and provide a discussion of the limitations and the necessary boundary conditions for maximum trapping efficiency. The photorefractive crystal is utilized as bottom part of a PDMS channel in order to demonstrate two-dimensional dielectrophoretic trapping in a microfluidic system.

OCIS codes: (350.4855) optical manipulation; (160.3730) lithium niobate; (190.5330) photorefractive optics

References and links

1. G.M. Whitesides, "The origins and the future of microfluidics", Nature **442**(7101), 368-373 (2006)
2. C.H Ahn, J.W Choi, G. Beaucage , J.H. Nevin, J.B. Lee, A. Puntambekar, and J.Y Lee, " Disposable Smart lab on a chip for point-of-care clinical diagnostics", Proc. IEEE, **92**(1), 154-173 (1998)
3. S.Y. Teh, R. Lin, L.H. Hung, and A.P.Lee, "Droplet microfluidics", Lab-on-a-Chip **8**(2), 198-220 (2008)
4. D. Psaltis, S.R. Quake, and C.H. Yang, "Developing optofluidic technology through the fusion of microfluidics and optics", Nature **442**(7101), 381-386 (2006)
5. D.M. Pai and B.E. Springett, "Physics of Electrophotography", Rev. Mod. Phys. **65**(1) , 163-211 (1993)
6. N. Ranjan, M. Mertig, G. Cuniberti, and W.Pompe, "Dielectrophoretic Growth of Metallic Nanowires and Microwires: Theory and Experiment", Langmuir **26**(1), 552-559 (2010)
7. H. Morgan, "Large-area travelling wave dielectrophoresis particle separator", J. Micromech. Microeng. **7**(2), 65-70 (1997)
8. H. Morgan, M.P. Hughes, and N.G. Green, "Separation of submicron bioparticles using dielectrophoresis", Biophys. J., **77**(1), 516-525 (1999)
9. P.R.C. Gascoyne and J. Vykoukal, "Particle separation by dielectrophoresis", Electrophoresis **23,** 1973-1983 (2002)
10. A. Ashkin, "Acceleration and trapping of particles by radiation pressure", Phys. Rev. Lett. Vol. **24**(4), 156-159 (1970)
11. A. Jonas and P. Zemanek, "Light at work: The use of optical forces for particle manipulation, sorting, and analysis", Electrophoresis **29**, 4813-4851 (2008)
12. P.Y. Chiou, A.T. Ohta, and M.C. Yu, "Massively parallel manipulation of single cells and microparticles using optical images", Nature **436**, 370-372 (2005)
13. V.M Petrov, C.Denz, A.V. Shamray, M.P. Petrov, and T. Tschudi, "Electrically controlled volume LiNbO3 holograms for wavelength demultiplexing systems", Opt. Mat. **18**(1), 191-194 (2001)
14. V.V. Krishnamachari, O. Grothe, H. Deitmer, and C. Denz, "Novelty filtering with a photorefractive lithium-niobate crystal", Appl. Phys. Lett. **87**(7), 071105 (2005)
15. M. Woerdemann, F. Holtmann, and C. Denz, "Holographic phase contrast for dynamic multiple-beam optical tweezers", J. Opt. A: Pure Appl. Opt. **11**(3), 034010 (2009)
16. P. Yeh, "Introduction to Photorefractive Nonlinear Optics", Wiley Interscience, 1993

17. H.A. Eggert, F.Y. Kuhnert, K.Buse, J.R. Adleman, and D. Psaltis, "Trapping of dielectric particles with light-induced space-charge fields", Appl. Phys. Lett. **90**(24), 241909 (2007)
18. K.H. Bhatt and O.D. Velev, "Control and modeling of the dielectrophoretic assembly of on-chip nanoparticle wires", Langmuir **20**(2), 467-476 (2004)
19. D.C. Duffy, J.C. McDonald, O.J.A. Schueller, and G.M. Whitesides, "Rapid prototyping of microfluidic systems in poly(dimethylsiloxane)", Analytical Chemistry, **70**, 4974–4984 (1998)
20. H.A. Pohl, "Some effects of nonuniform fields on dielectrics", J. Appl. Phys. **29**(8), 1182-1188 (1958)
21. T. B. Jones, "Electrokinetics of Particles", Cambridge University Press, 1995
22. S. Grilli and P. Ferraro, "Dielectrophoretic trapping of suspended particles by selective pyroelectric effect in lithium niobate crystals", Appl. Phys. Lett. **92**(23), 232902 (2008)
23. P. Rose, B. Terhalle, J. Imbrock, and C. Denz, "Optically induced photonic superlattices by holographic multiplexing", J. Phys. D: Appl. Phys. **41**(22), 224004 (2008)
24. A. Ashkin, G.D. Boyd, J.M Dziedzic, R.G. Smith, A.A. Ballman, J.J. Levinstein, and K.Nassau, "Optically-induced Refractive Index Inhomogeneities in LiNbO3 and LiTaO3", Appl. Phys. Lett. **9**(1), 72+ (1966)
25. B. Sturman and V. Fridkin, "The Photovoltaic and Photorefractive Effects in Noncentrosymmetric Materials", Gordon & Breach Science Publishers, 1992
26. H. Kogelnik, "Coupled Wave Theory for Thick Hologram Gratings", Bell Sys. Tech. J. **48**, 2909+ (1969)
27. P. Günter, J.-P. Huignard, "Photorefractive Materials and Their Applications 1: basic effects", Springer, 2006
28. P.M. Kruglyakov, "Hydrophile - Lipophile Balance of Surfactants and Solid Particles", Elsevier, 2000
29. N. Markarian, M. Yeksel, B. Khusid, K. Farmer, and A. Acrivos, "Limitations on the scale of an electrode array for trapping particles in microfluidics by positive dielectrophoresis", Appl. Phys. Lett. **82**(26), 4839-4841 (2003)
30. X.Z. Zhang, J.Q Wang, B.Q. Tang, X.H. Tan, R.A. Rupp, L.T. Pan, Y.F. Kong, Q. Sun, and J.J. Xu, "Optical trapping and manipulation of metallic micro/nanoparticles via photorefractive crystals", Opt. Expr. **17**(12), 9981-9988 (2009)
31. P. Yeh, "Fundamental Limit of the Speed of Photorefractive Effect and its Impact on Device Applications and Material Research", Appl. Opt., **26**, 602–604 (1987)

1. Introduction

Microfluidics has revolutionized the field of on-site diagnostics by reducing both cost and reactant consumption [1,2,3] as well as opened new connections between optics and fluidics [4]. An important task in this field is the manipulation of particles on the micro- and nanoscale, which typically involves strong electric fields. Dielectrophoresis has already proven to be a powerful method in a variety of fields, ranging from document reproduction in copier machine [5] to the controlled growth of micro- and nanostructures [6] as well as particle transport and separation [7-9]. Due to the static nature of the external electrodes, this concept does not allow dynamic readjustment of the experimental setup. This shortcoming can be overcome by optical approaches. Optical tweezers have been known since the early 70s [10] and have today become a well-established tool for manipulating particles in the field of biological research [11]. On the one hand, they offer precise control, but on the other hand lack high throughput, since high laser powers are required. *Chiou et al*. have demonstrated the combination of optical configuration and dielectrophoretic particle manipulation in a dynamic setup with optically-controlled virtual electrodes [12]. This method is flexible, but still dependent on an external voltage supply. Another way to generate large electric fields is possible through the use of a photorefractive crystal. Due to their electrooptic properties, these materials have found wide application in holographic data storage [13], novelty filtering devices [14] or optical tweezers [15]. The nonlinear conversion from optical patterns to electric field modulations allows an electrode-less approach to dielectrophoresis. Inside a photorefractive crystal, the redistribution of charge carriers leads to the formation of virtual electrodes and highly modulated fields [16]. *Eggert et al*. suggested the exploitation of these strong electric fields for dielectrophoretic particle trapping [17]. Until now, only one-dimensional photorefractive trapping has been demonstrated, however, for many applications,

such as controlled particle growth, two-dimensional particle alignment is desirable [18]. Since many microfluidic applications are based on disposable polydimethylsiloxane (PDMS) chips [19], it is furthermore the aim of this contribution to demonstrate that the combination of two-dimensional particle trapping in a photorefractive material and the application of this technique to a PDMS continuous-flow environment are possible.

2. Dielectrophoretic trapping

Dielectrophoresis describes the movement of matter in highly inhomogeneous electric fields. In contrast to electrophoretic forces, that show a linear dependence on the field and act only on charged particles, dielectrophoretic (DEP) forces act on any polarizable matter.
For a spherical particle in a surrounding medium, they can be calculated from [20, 21]

$$F_{DEP} = 2\pi r^3 \varepsilon_m \,\mathrm{Re}\left[\alpha(\omega)\right] \nabla E^2 \tag{1}$$

with r as the particle radius, ε_m as the relative dielectric permittivity of the surrounding medium and E as the electric field.
The sign and magnitude of the DEP force is dependent on the Clausius-Mossotti factor α, which is defined as [21]

$$\alpha(\omega) = \frac{\varepsilon_p(\omega) - \varepsilon_m(\omega)}{\varepsilon_p(\omega) + 2\varepsilon_m(\omega)} \tag{2}$$

with ε_p as the permittivity of the particles. Depending on the sign of α in Eq. (2), one can distinguish between positive DEP ($\alpha > 0$) - particles are attracted towards regions of high field strength, and negative DEP – matter is repulsed and moves to regions of minimal field strength. As can be seen from Eq. (1), for the DEP force to have a significant effect on particles, the gradient of the electric field has to be very high. Such a scenario can be realized by the application of external electrodes, which is a well-approved technique [6-9], but lacks flexibility and reconfigurability. Photorefractive materials offer a connection between photonics and electronics by converting an intensity modulation into an electric field modulation. *Eggert et al.* have proposed and demonstrated the use of a $LiNbO_3$ crystal and the exploitation of the strong electric fields that occur upon non-uniform illumination by virtue of the bulk photovoltaic effect [17]. *Grilli and Simoni* have demonstrated that that the pyroelectric fields occurring during temperature changes in periodically poled lithium niobate (PPLN) can also be used for positive as well as negative DEP [22]. The previously mentioned contributions demonstrated one dimensional modulation or utilized previously poled crystals. The structuring via periodic poling remains unflexible due to their fixed and necessarily periodic structure. Two-dimensional modulation of a photorefractive material, however, offers dynamic reconfiguration of trapping patterns. This modulation could be done by the interference of plane waves, but this approach is limited to periodic structures and involves a lot of experimental work because it requires the precise adjustment of at least 3, often more plane waves for a two-dimensional modulation. The combination of high flexibility and all-optical two-dimensional structuring can be elegantly achieved by the use of an amplitude modulating spatial light modulator (ASLM), which has already been utilized for the induction of transversely modulated photonic structures [23]. In this case, possible patterns are only limited by the ASLM resolution and, with certain materials, the crystal geometry.

3. Two-dimensional structuring of a lithium niobate crystal

Photorefractive crystals offer the possibility to exert high electric field strengths under non-uniform illumination, an effect first discovered by *Ashkin et al.*[24]. The modulation of the electric fields in these materials is based on a redistribution of excited charge carriers by virtue of different well-understood effects [16]. In particular, the modulation in $LiNbO_3$ is due to the photovoltaic (PV) effect in the material and the magnitude of the electric fields can be on the order of kV/mm [17, 25]. In the present experiments, a lithium niobate crystal (13 x 15 x 2 mm^3) with 0.05 wt % Fe dopant concentration is used. In a preliminary diffraction experiment, the field strength for a modulation along the c-axis was calculated from the diffraction efficiency to be 1.6 kV/mm [26]. Perpendicular to the c-axis, the elements of the photovoltaic tensor are either zero or very small (depending on the polarization) [27] and the contribution from the diffusion field is one order of magnitude smaller than the PV field and can be neglected [25].

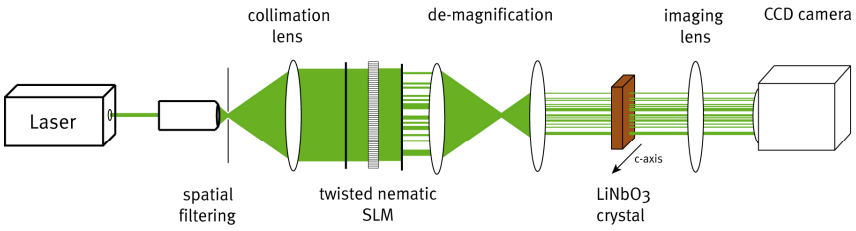

Fig.1: Setup for structuring a photorefractive crystal using an amplitude modulator

The setup for light-induced two-dimensional structuring of a photorefractive material using an ASLM is sketched in Fig. 1. It consists of a frequency-doubled Nd:YAG laser (λ = 532nm), whose beam is expanded and spatially filtered for homogeneous illumination. Amplitude modulation is achieved through the use of a phase-only modulator (resolution: 800 x 600 pixels) between two polarizers in parallel orientation. Its pixels consist of twisted nematic cells, which not only perform a phase-modulation but also turn the input polarization dependent on the gray value (and thus the voltage) applied to a cell (Schadt-Helfrich cell operated in *normally-black mode*). The modulator accepts gray values from 0 (dark pixel) to 255 (bright pixel). The real achievable modulation contrast is 70. In contrast to the interference of plane waves that can also create two-dimensional intensity modulations, the SLM enables the induction of purely arbitrary patterns, only limited by its resolution.

Since the SLM is large in diameter, its image is demagnified in front of the crystal. By this demagnification, the incident light intensity is increased and the time necessary for a sufficient charge redistribution is reduced. In order to check the quality of the pattern-inducing wave, a CCD camera is placed behind the crystal. The induction of patterns is done with a mean intensity of 40 mW/cm^2 in approximately 30 minutes. After structuring, the crystal is dusted with the particles to be trapped. After five seconds, the untrapped rest is blown off. Graphite particles with a broad size distribution of 5-20 µm and dielectric constant of $\varepsilon_p = 15$ are used in the experiments, which means that surrounded by air, they will be subject to positive DEP with a Clausius-Mossotti factor of $\alpha = 0.824$. The liquid medium for the microfluidic experiments is tetradecane, an oil with a dielectric constant of $\varepsilon_m = 2.0$ [28], which translates into $\alpha = 0.684$. After each experiment, the crystal is cleaned with isopropanole and heated to ensure no gratings from previous experiments are left.

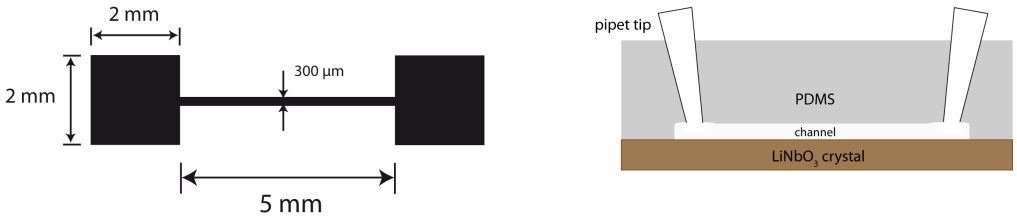

Fig.2: PDMS channel geometry (left) and sketch of assembly on photorefractive crystal (right); the channel height in reservoirs and straight section is 50 µm

Channels of polydimethylsiloxane (PDMS) fabricated by replica molding are used for the experiments concerning the microfluidic part [19]. PDMS is the microfluidic material of choice due to its low Young's modulus and good transparency in the visible range. Furthermore, it is self-adherent to many important materials like glass or photorefractive crystals. Therefore, sealing by oxygen plasma is not absolutely necessary. Fig. 2 shows the basic layout of the channel with two large end reservoirs and a straight channel section of smaller diameter. The channel end reservoirs are connected to pipet tips for easier access. The channel is filled with a 0.5 wt.% suspension of graphite particles in tetradecane. A flow is induced by different filling heights of the pipet tips, hence by low pressure of approximately 0.29 mPa.

4. DEP trapping in air

Before starting with the actual trapping experiments with graphite, a phase-contrast image of the crystal after optical structuring is taken. In these images (Fig. 2), the induced structures (triangular and tilted square pattern) are clearly visible and one can assure that the refractive index modulation in the crystal coincides with the pattern-inducing wave in terms of shape as well as in size (triangle: 300 µm; square: 330 µm). A higher frequency modulation of the refractive index from the relatively large pixel structure of the modulator (pixel pitch: 32 µm) is visible, causing the bright areas to have a stripe-like sub-pattern. This stripe pattern is caused by the anisotropy of the $LiNbO_3$ crystal which generates large electric fields along its c-axis due to the bulk PV effect. As can be seen in the phase-contrast images, the high PV fields lead to a large contrast for modulations along the c-axis but to negligible contrast perpendicular to it.

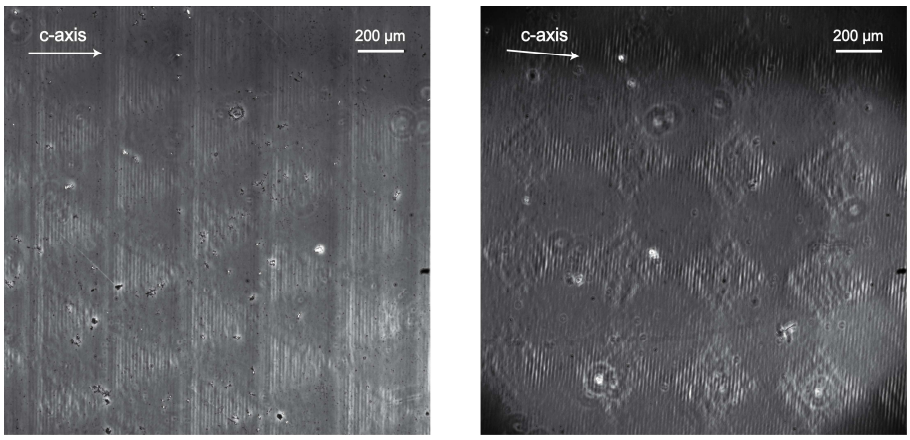

Fig.3: Contrast enhanced phase-contrast images of the triangular (left) and tilted square pattern (right); total field of view 1.86 mm x 1.85 mm; stripe-like sub-pattern is due to pixel structure of the SLM device

The result for the trapping of graphite particles in Fig. 4 shows clearly the extension of DEP particle alignment to complex two-dimensionally modulated structures. The general trapping efficiency is large, leading to expanded stripes – up to 100 µm - of aligned graphite at each dark/bright interchange in the pattern, which effectively leads to a doubling of the spatial frequency [17]. An interesting observation is that in the corners of the pattern, no particles are captured, although in the phase-contrast images (cf Fig. 3) no irregularities can be identified. The most likely explanation is that in the corner regions, while the field gradients are very high, dipole-dipole interactions between ionized particles affect the DEP trapping.

Markarian et al. have further investigated the geometrical scale effects and stated that for the dipole-dipole effects to be negligible, the "electrode" pattern, i.e. in this case the transition area between high and low refractive index areas, should satisfy the condition [29]

$$F_{DD} / F_{DEP} = 6\alpha \left(\frac{r}{d} \right)^3 << 1 \tag{3}$$

with d as the spacing between electrodes. While for the middle sections of the edges, $F_{DD} / F_{DEP} \approx 10^{-3}$, in the corners this ratio increases dramatically since the electrode distance decreases. The fact that these areas are diversely pronounced is due to the broad size distribution of the graphite particles.

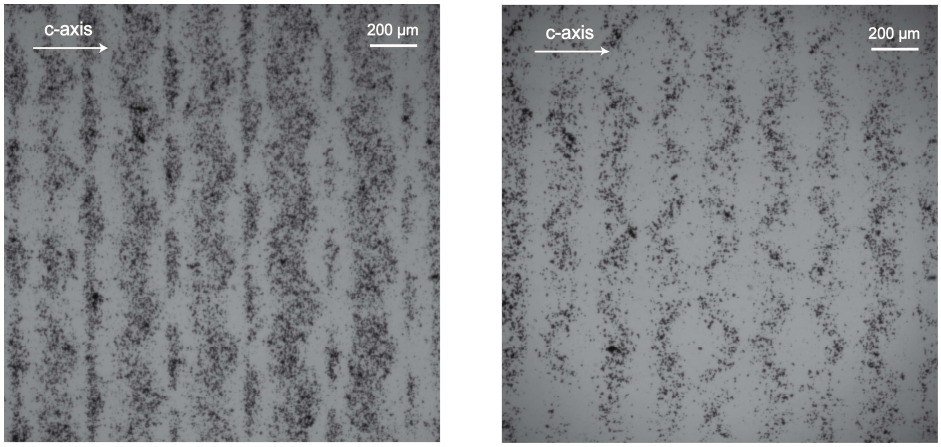

Fig.4: Graphite particles trapped on the surface of the $LiNbO_3$ crystal in triangular and tilted square geometry. In the corners of the pattern, the trapping efficiency reduces to zero, most likely due to dominating dipole-dipole interactions between particles.

The use of an ASLM enables the induction of non-periodic trapping patterns. Fig. 5 shows such an arbitrary trapping situation. The modulation perpendicular to the c-axis does not produce sufficient fields for particle trapping [17], another hint that the electric fields are generated by the PV effect along the c-axis of the material. Additionally, the result allows an estimation of the minimum angle, that an edge in a trapping configuration should be inclined to the c-axis. Looking at the letters in Fig. 5, one can state that an angle of more than approx. 30° must be sustained for a high trapping efficiency. Furthermore, the designer of a trapping pattern must decide if the previously described trapping at each dark/bright interchange is desired or, if this is not the case, modify the pattern accordingly.

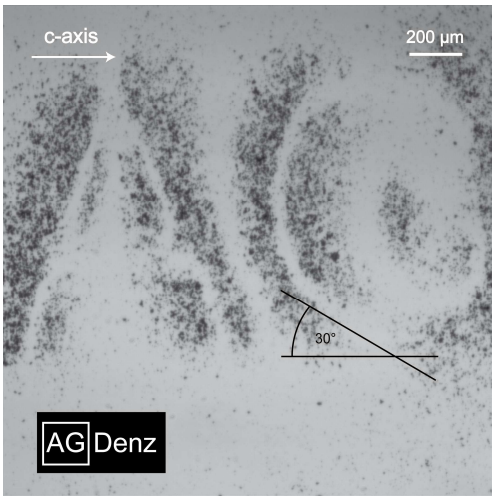

Fig. 5: Trapped graphite particles at the borders of the lettering "AG Denz" (black box). Image shows the letters A and G and illustrates the reduced trapping efficiency for the modulation perpendicular to the c-axis. The continuous transformation from perpendicular to parallel modulation in the letter G allows for an estimation of the necessary angle between pattern and c-axis.

6. Trapping in a PDMS microchannel

To demonstrate the feasibility of the technique for possible microfluidic applications, the optically-structured $LiNbO_3$ crystal is attached to a PDMS half-channel and filled with a suspension of graphite particles (5-20 µm) in tetradecane. Fig. 6 shows a section of the channel 30 seconds after it has been filled. Enough particles are captured to visualize the square pattern, which clearly demonstrates that particle alignment in a microfluidic environment is possible. Again, in the corners of the squares, the trapping efficiency is reduced but due to the continuous flow in the channel, there is a much higher probability that smaller particles, for which the dipole-dipole interactions are negligible, arrive in these areas.

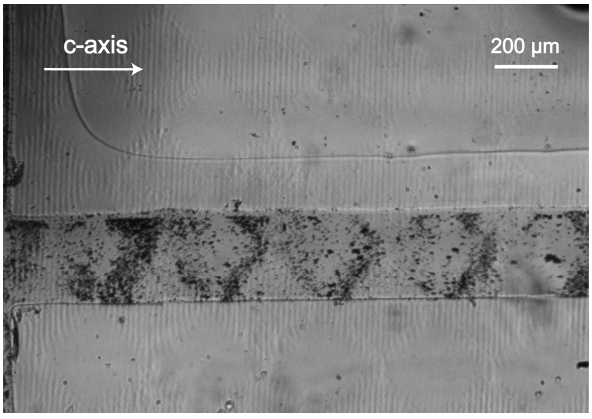

Fig. 6: Bright field image of two-dimensional particle trapping in a 300 x 50 µm PDMS microchannel after 30 seconds of particle alignment; note the strong visibility of the refractive index modulation

The theoretical lower resolution limit for the trapping structure is dependent on the wavelength used for pattern storage and the refractive index of the material and can be as low as 54 nm [30] in $LiNbO_3$. In any case, the inequality Eq. (3) should be fulfilled for efficient particle trapping, which imposes an upper limit on the particle size. Assuming that the quantity 6α is on the order of one, the radius of the particle should be one order of magnitude smaller than the electrode spacing. A lower limit arises due to the fact that the DEP force scales with the cube of the particle radius. It is therefore difficult to trap particles significantly smaller than 1 μm [12].

Limitations may arise due to the use of lithium niobate as the suface material. High electric fields are primarily by virtue of the bulk photovoltaic effect, which is only strong enough for particle tracking along a distinguished axis. Hence, not all conceivable trapping configurations are possible. An amplitude modulation perpendicular to the c-axis of the crystal will not generate sufficiently large fields for particle capturing. The second restriction when using $LiNbO_3$ is due to the large time constants of the photorefractive effect. However, these restrictions are only caused by the use of lithium niobate as the surface material. The configuration in general is not limited to the use of a particular photorefractive material. Faster photorefractive materials like $BaTiO_3$ or BSO could also be utilized for this approach. Depending on the laser power, $BaTiO_3$, allows time constants down to 100 ms [31].

7. Conclusion and outlook

We have demonstrated two-dimensional, optically induced particle trapping on a lithium niobate crystal in different complex trapping configurations. The trapping in square and triangle lattices as well as an arbitrary lettering and its feasibility in a PDMS microchannel were presented. The only experimental requirement is a twisted-nematic amplitude spatial light modulator or any other kind of amplitude modulating device. This configuration allows a high degree of flexibility and the extension to patterns with a finer substructure is straight-forward using an ASLM with higher resolution. The next step is the utilization of faster materials and the integration of optical structuring and microfluidic environment into a single setup to establish a dynamic microfluidic particle manipulation system.

Acknowledgement

The authors gratefully acknowledge financial support from the Deutsche Forschungsgemeinschaft in the frame of the German-Chinese transregional research project TRR61.